AIAA JOURNAL
Vol. 41, No. 11, November 2003

Effect of Vibrational Nonequilibrium on Hypersonic Double-Cone Experiments

Ioannis Nompelis* and Graham V. Candler†
University of Minnesota, Minneapolis, Minnesota 55455
and
Michael S. Holden‡
Calspan—University at Buffalo Research Center, Buffalo, New York 14225

Recent numerical simulations of hypersonic double-cone experiments overpredict the heat-transfer rate to the model by about 20%. We present a systematic analysis of the experimental facility and the physical modeling to explain this discrepancy. Nozzle flowfield simulations are used to investigate the effect of vibrational nonequilibrium in the test section. These simulations show that the vibrational modes of the nitrogen gas freeze near the nozzle throat conditions, resulting in an elevated vibrational temperature in the test section. This lowers the kinetic energy flux, reducing the heat transfer to the model. The effect of slip boundary conditions is also studied, and it is shown that weak accommodation of vibrational energy at the surface further reduces the heat-transfer rate to the model. The combination of these two effects brings the predicted heat-transfer rate into agreement with the experiments. In addition, weak flow nonuniformity in the test section is shown to slightly modify the predicted separation zone, further improving the agreement.

Introduction

THE interaction between shock waves and boundary layers is a phenomenon frequently encountered in hypersonic flight. Shock interactions cause high localized heat-transfer rates on the vehicle surface, and they can alter the aerodynamic characteristics of the vehicle. In addition, their large range of length scales makes them challenging to simulate with computational fluid dynamics. One means of generating a stable, strong shock interaction is with a double-cone geometry in a hypersonic flow. As seen in Fig. 1, if the first cone is chosen with a cone angle below the detachment angle and the second cone has an angle above the detachment angle, a complex flow is formed. The attached shock interacts with the detached shock, resulting in a transmitted shock that impinges on the boundary layer. This separates the flow in the vicinity of the corner between the cones; the separation then produces a shock wave that strengthens the attached shock, further altering the flowfield. The coupling between the shock waves and the separation zone makes this flow very challenging to simulate with computational fluid dynamics. Inaccuracies in the physical models and weaknesses in the numerical method result in easily measured differences in the surface properties. This sensitivity makes the double-cone flow an ideal code validation test case.

Previous work has shown that to simulate a double-cone flow correctly, a high-quality numerical method must be used with a large number of grid points. For example, simulations of double-cone flows in the Princeton University Mach 8 Tunnel were successful with very fine grids ($\frac{1}{2}$ million point grids) for low second cone angles where transition was unimportant.[1] However, attempts to reproduce double-cone and double-wedge flows at high enthalpy were largely unsuccessful.[2,3]

Recently, a new set of double-cone experimental data was taken at well characterized hypersonic conditions in the Calspan—University at Buffalo Research Center (CUBRC) Large Energy National Shock Tunnel (LENS).[4] These experiments used a large model with many surface-mounted heat-transfer and pressure transducers. Nitrogen was used as the test gas to minimize the effects of chemical reactions, and the experiments were done at low pressure to ensure laminar boundary layers and shear layers. These experiments have been used as validation cases for the NATO Research and Technology Organization (RTO) Working Group 10 validation activities[5–7] and other research groups have simulated these flows,[8–11] culminating in a blind code validation study in January 2001 (Ref. 7).

The key results of the code validation study are summarized in Fig. 2, which plots our computed surface pressure and heat-transfer rate against the experimental data for two of the double-cone test cases. The other continuum computational simulations were very similar to the plotted results.[8–11] In general, the computations agree with the experiments: the pressure is constant on the first cone, there is a large pressure rise in the separation region, and the magnitude of the pressure overshoot caused by the shock interaction is captured. The heat-transfer results are also generally good, but there is a notable difference on the first cone where the heat transfer is overpredicted by about 20%. This is substantially beyond the quoted 5% uncertainty in the measurements[4]; this difference was obtained by almost all of the other simulations. The simulations assume that the flow is laminar, which is consistent with the experiments. If the flow were transitional or turbulent, the simulations would underpredict the measurements. Also, we expect the flow to be laminar because the Reynolds number based on the freestream conditions and model diameter is at most 40, 900 for the cases considered.

Therefore, the purpose of this paper is to study the source of the discrepancy in the computed heat-transfer rate on the first cone. In previous work[10] we considered the effects of possible finite nose-tip bluntness, model misalignment, and uncertainties in chemical reaction rates. However, these effects cannot explain the differences in the heat-transfer rate, and thus in this paper we assess the accuracy of the nominal test-section conditions from Ref. 4 by using computational fluid dynamics (CFD) to compute the flow in the LENS facility nozzle including the effects of vibrational nonequilibrium.

Presented as Paper 2002-0581 at the AIAA Aerospace Sciences Meeting, Reno, NV, 14–17 January 2002; received 14 January 2002; revision received 10 June 2003; accepted for publication 30 June 2003.

*Graduate Research Assistant, Aerospace Engineering and Mechanics and Army HPC Research Center, 110 Union Street SE; nompelis@aem.umn.edu. Student Member AIAA.

†Professor, Aerospace Engineering and Mechanics and Army HPC Research Center, 110 Union Street SE. Associate Fellow AIAA.

‡Program Manager, Aerooptics Evaluation Center. Associate Fellow AIAA.

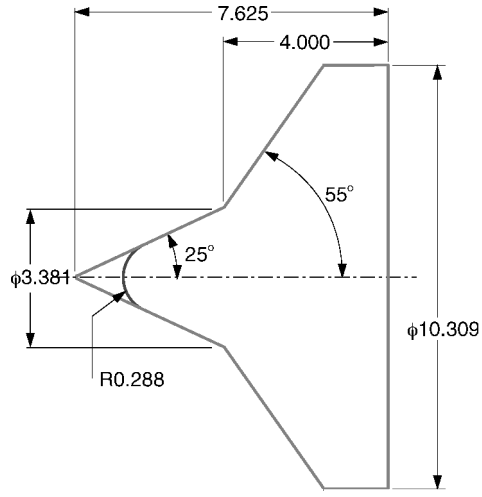

Fig. 1a Schematic of the double-cone wind-tunnel model; sharp and blunted fore-cone pictured (dimensions in inches).

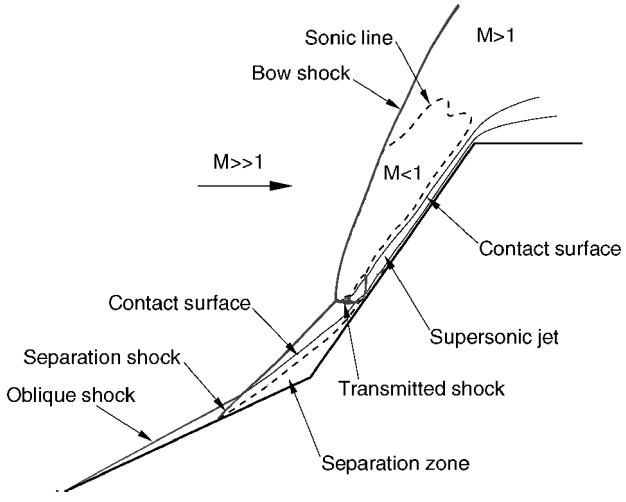

Fig. 1b Schematic of the double-cone flow.

We also investigate the accuracy of the conventional no-slip boundary condition for these relatively low-density flows. Finally, we use our computed test-section conditions to study the effect of slight freestream nonuniformity on the computed separation zone size. Including all of these effects results in improved agreement between the computations and experiments.

Numerical Method

In this work we simulate the flow of nitrogen that is vibrationally relaxing and is allowed to dissociate. We solve a separate mass conservation equation for each of the two species, namely atomic and diatomic nitrogen using Park[12] dissociation rates. To account for vibrational nonequilibrium, a separate vibrational energy conservation equation is solved along with the mass, momentum, and total energy equations. We use a simple harmonic oscillator with the Landau–Teller model,[13] with Millikan and White rates.[14] The mixture viscosity and thermal conductivity are computed from Blottner et al.[15] fits using Wilke's semi-empirical mixing rule.[16] Mass diffusion is modeled with a constant Lewis number and a single diffusion coefficient computed from Blottner fits. The methods have been applied with success to a number of hypersonic low-density flows.

We solve the conservation equations over the axisymmetric domain using a fully implicit finite volume solver based on the data parallel line-relaxation method of Wright et al.,[17] which uses second-order-accurate modified Steger–Warming inviscid fluxes.[18,19] The viscous fluxes are modeled with a second-order-accurate scheme.

At the flow enthalpy of interest, there is essentially no dissociation of nitrogen. The reservoir atomic nitrogen mole fraction is less

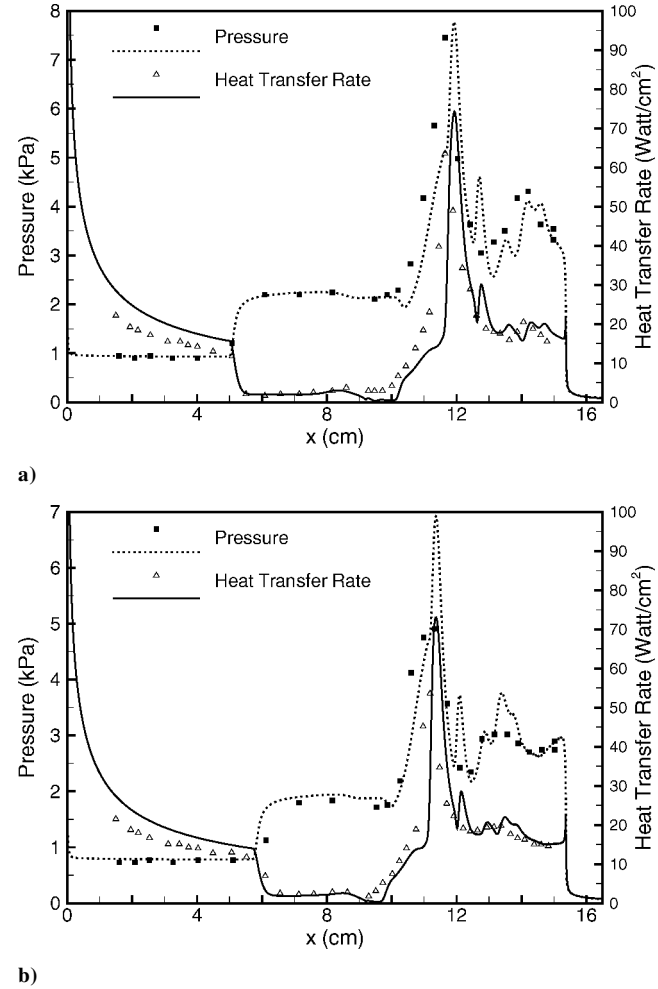

Fig. 2 Comparison of Navier–Stokes predictions of surface quantities with experimental data for a) run 28 and b) run 35.

than 1×10^{-5}, and thus our model is effectively pure vibrationally excited N_2.

The quality of the numerics used to simulate the double-cone flows is very important. This is the subject of a separate study[20] that shows that many second-order-accurate upwind methods can be used to simulate these flows, provided that the computational grid is large enough and is carefully designed. Figure 3 summarizes the results of a grid-convergence study, in which we simulate the flow of a perfect gas over the double-cone at nominal run 35 conditions. From this study that uses the modified Steger–Warming method, we see that the heat-transfer rate computed on the 1024×512 and 2048×1024 grids are virtually identical. Thus, the results obtained on the 1024×512 grid are converged, and all results presented in this paper were obtained on this grid, unless otherwise stated.

The study by Gaitonde et al.[21] shows similar grid convergence for this flow. They also conduct a careful time-convergence study and show that the solution does not converge until at least 100 characteristic flow times have been computed. This relatively long timescale allows the separation zone to become fully established. They define the characteristic time to be the time required to travel the length of the double-cone model at the freestream velocity. Our simulations are consistent with their findings, and we simulate our flows to a minimum of 150 flow times.

Vibrational Nonequilibrium

The specification of the freestream conditions is an important aspect of hypersonic flow experiments. In a reflected shock hypersonic wind tunnel such as LENS, high temperature and pressure gas is expanded from the reservoir conditions through a contoured nozzle to high Mach number. It is well known that the vibrational modes of the gas can freeze near the nozzle throat conditions. Vibrational

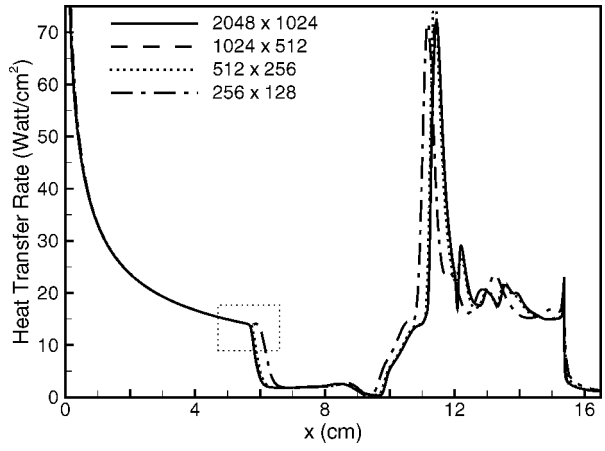

Fig. 3a Heat-transfer rate for a perfect gas simulation computed on four different grids.

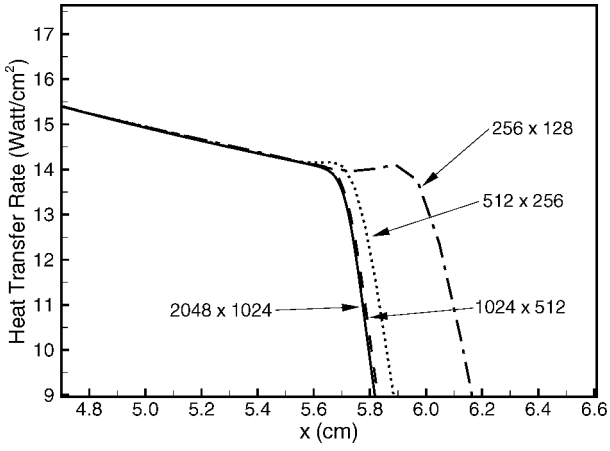

Fig. 3b Enlargement near the separation point.

freezing is particularly important in nitrogen at relatively low pressure reservoir conditions, as is the case in the present experiments. Roy et al.[11] expressed concern that vibrational freezing could affect the test conditions in the present experiments.

In this section we discuss how vibrational freezing affects the inferred test conditions in the LENS facility. In the experiment, calibration runs are performed before the tests to verify the uniformity of the flow section. Subsequently, the actual experiments are performed at the same nominal conditions as the calibration runs. In an impulse facility such as LENS, the pressure and enthalpy in the reservoir region behind the reflected shock are known. The pitot pressure in the test section can be measured easily, as well as the heat-transfer rate to a reference probe. Additional pitot-pressure measurements are made during the experiment to verify that the test conditions are consistent with the calibration run.

To determine the freestream conditions, a quasi-one-dimensional code is run using the measured reservoir stagnation conditions. Although the exact geometrical specification of the nozzle is known, the effective area ratio is not known because of the wall boundary-layer displacement. Therefore, the code is run to the point where the computed pitot pressure matches the pressure measured by the pitot probe. Then, the test conditions are taken to be those given by the quasi-one-dimensional code. This analysis assumes vibrational equilibrium during the expansion and has been successfully used for a long time but usually in air at pressures higher than considered in the present experiments.

To illustrate how the freestream conditions are inferred, consider the Rayleigh pitot-pressure formula

$$\frac{p_{02}}{p_\infty} = \frac{\gamma+1}{2}M_\infty^2\left(\frac{\gamma+1}{2}M_\infty^2 \Big/ \frac{2\gamma}{\gamma+1}M_\infty^2 - \frac{\gamma-1}{\gamma+1}\right)^{1/(\gamma-1)}$$

which in the hypersonic limit reduces to

$$p_{02} = \frac{\gamma+1}{2}\left[\frac{(\gamma+1)^2}{4\gamma}\right]^{1/(\gamma-1)} p_\infty M_\infty^2$$

$$= \frac{\gamma+1}{2\gamma}\left[\frac{(\gamma+1)^2}{4\gamma}\right]^{1/(\gamma-1)} \rho_\infty u_\infty^2$$

where p_{02} is the measured pitot pressure and ∞ denotes the freestream conditions. Thus, the pitot pressure is effectively a measurement of the kinetic energy per unit volume in the freestream.

Now consider an ideal, adiabatic expansion from the reservoir to hypersonic conditions. The total enthalpy of the reservoir is converted to freestream kinetic energy conserved according to

$$h_0 = C_p T_\infty + \tfrac{1}{2}u_\infty^2 \simeq \tfrac{1}{2}u_\infty^2$$

where we have assumed that $\frac{1}{2}u_\infty^2 \gg C_p T_\infty$. Therefore, given the reservoir enthalpy we have the value of u_∞^2 in the inviscid portion of the nozzle flow. Then, with a measurement of the pitot pressure we effectively measure the freestream density for the ideal expansion.

Now consider what happens if there is vibrational energy frozen in the flow during the expansion. We have

$$\tfrac{1}{2}u_\infty^2 \simeq h_0 - e_v^*$$

where e_v^* is the vibrational energy per unit mass frozen in the flow. Thus, the kinetic energy will be lower than in an ideal expansion, and to obtain the same measured pitot pressure the freestream density must be larger. Thus, the effect of vibrational freezing in the nozzle is to lower the axial velocity and increase the density relative to an equilibrium analysis. To first order, the surface-pressure scales with $\rho_\infty u_\infty^2$ and the heat-transfer rate with $\rho_\infty u_\infty^3$. Thus, we do not expect vibrational freezing to affect the measured surface pressure, but it should reduce the measured heat-transfer rate caused by the lower value of u_∞.

In this analysis we have assumed that the Rayleigh pitot-pressure formula is valid under conditions of vibrational nonequilibrium. We have simulated the flow over the pitot probes used in the experiments using a finite rate relaxation model for nitrogen. These calculations show that under the conditions of interest the Rayleigh pitot-pressure formula gives the correct value of pitot pressure (to within four digits of accuracy), and the preceding analysis is valid.

Nozzle Flow Simulations

The preceding elementary analysis shows that vibrational freezing reduces the measured heat-transfer rate. However, a more complete analysis is required to determine how much vibrational freezing occurs and to assess the additional nonideal effects in the nozzle flow. Thus, we have performed a series of CFD simulations of the nozzle flows. In these simulations we have used the numerical method discussed earlier with the Baldwin–Lomax turbulence model[22] for the nozzle wall boundary layer.

The nozzle grids are constructed directly from the CAD files of the nozzle contours. Typical grids use 1788 points in the axial direction and 128 points in the surface normal direction, with stretching at the surface. The nozzle throats are elongated, making the specification of the sonic line difficult. Thus, the flow is computed from the constant diameter driven tube section, through the throat, and to the test section. Thermochemical equilibrium was assumed at the inflow, and subsonic inflow conditions were implemented so that total enthalpy is conserved in the computed flow.

Initial simulations of the nozzle flow were discouraging, with the centerline pitot pressure significantly overpredicted. This is caused by the turbulence model overpredicting the boundary-layer displacement thickness at the nozzle exit plane. Previous simulations of hypersonic nozzles showed significant variations in the computed test-section conditions depending on the choice of the turbulence model, with the Baldwin–Lomax model typically

Table 1 Nominal and computed test-section conditions for run 35 reservoir conditions

Parameter	Nominal	Nonequilibrium
T_∞, K	138.9	98.27
$T_{v\infty}$, K	138.9	2562
ρ_∞, g/m^3	0.5515	0.5848
u_∞, m/s	2713	2545
M_∞	11.30	12.59
$\rho_\infty u_\infty^2$, Pa	4059	3788
$\rho_\infty u_\infty^3$, W/cm^2	1101	964

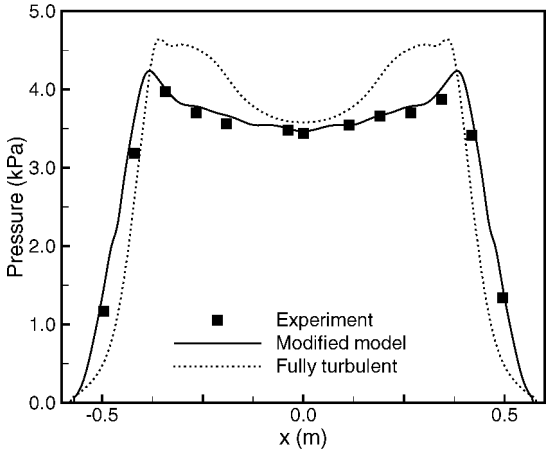

Fig. 4 Run 1302 (calibration for run 35) pitot pressure in the nozzle exit plane compared with nozzle computations.

giving intermediate values for the boundary-layer displacement thickness.[23]

The strong favorable pressure gradient in the nozzle reduces the effect of turbulent transport through the boundary layer, reducing the rate of boundary-layer growth. This mechanism is not included in any algebraic turbulence models, and we were thus forced to perform parametric studies to match the measured pitot-pressure profile. We found that by reducing the effect of the turbulence model as the flow expands it is possible to obtain good agreement with the calibration measurements.

For example, Fig. 4 plots the measured pitot pressure for the calibration run for run 35 ($p_0 = 3.55$ MPa, and $h_0 = 3.71$ MJ/kg) with the results of two nozzle simulations. The calculation with fully turbulent boundary layer overpredicts the displacement thickness, resulting in a smaller effective area ratio and higher pitot pressure. However, when we assume that the turbulence model is not active downstream of 2.2 m from the throat the displacement thickness is reproduced. Thus we have effectively calibrated the turbulence model under the nozzle expansion conditions by matching the measured displacement thickness.

With this turbulence model calibration we ran a nozzle simulation with the actual run 35 reservoir conditions ($p_0 = 3.77$ MPa, and $h_0 = 3.83$ MJ/kg). From the simulation we obtain the freestream conditions at the test section. The results of this simulation are tabulated in Table 1 along with those obtained in Ref. 4 using the equilibrium quasi-one-dimensional analysis. Note that the vibrational temperature is predicted to freeze at 2562 K, which is close to the throat temperature. The resulting dynamic pressure and kinetic energy flux are also given. The computed value of the dynamic pressure is lower than that derived from the nominal conditions because we have matched the pitot-pressure profile, rather than a single mean value of pitot pressure. Also note that $\rho_\infty u_\infty^3$ is 12.4% lower in the nonequilibrium simulations because of the 6.7% lower value of pitot pressure and the 6.2% lower value of axial velocity. A similar analysis was carried out for run 28, and the results are given in Table 2. In this case the predicted pitot pressure is 2.5% higher, and the resulting kinetic energy flux is reduced by only 2.6%.

Table 2 Nominal and computed test-section conditions for run 28 reservoir conditions

Parameter	Nominal	Nonequilibrium
T_∞, K	185.6	140.0
$T_{v\infty}$, K	185.6	2589
ρ_∞, g/m^3	0.6545	0.7372
u_∞, m/s	2664	2538
M_∞	9.50	10.5
$\rho_\infty u_\infty^2$, Pa	4645	4749
$\rho_\infty u_\infty^3$, W/cm^2	1237	1205

Slip Boundary Conditions

In this section we consider noncontinuum effects and in particular the effect of partial accommodation of incident particles at solid boundaries. The standard Maxwell model[24] for velocity slip and temperature jump at the surface of the body is

$$v_{\rm ts} = \frac{2-\sigma}{\sigma}\lambda\left.\frac{\partial v_t}{\partial n}\right|_{\rm wall}$$

$$T_s - T_{\rm wall} = \frac{2-\sigma_T}{\sigma_T}\frac{2\gamma}{(\gamma+1)Pr}\lambda\left.\frac{\partial T}{\partial n}\right|_{\rm wall}$$

where $v_{\rm ts}$ and T_s are the tangential velocity and temperature at the surface (the slip conditions), $T_{\rm wall}$ is the temperature of the surface, λ is the mean free path, and σ and σ_T are the accommodation coefficients and are taken to be 0.85.

We must also model the possible jump of vibrational energy at the surface. This is done with a simple extension of the Maxwell model based on the approach of Ref. 25. The vibrational energy jump is

$$e_{\rm vs} - e_{\rm v\,wall} = \frac{2-\sigma_v}{\sigma_v}\lambda_v\left.\frac{\partial e_v}{\partial n}\right|_{\rm wall}$$

where σ_v is the accommodation coefficient for vibration and λ_v is the mean free path that characterizes transport of vibrational energy. Because the vibrational energy is not correlated with the translational energy modes, we use the value of mean free path for the transport of momentum, namely, $\lambda_v = \lambda = 2\mu/\rho\bar{c}$, where $\bar{c} = \sqrt{(8RT/\pi)}$ is the mean thermal speed of the gas. The value of the vibrational energy accommodation coefficient is not well known, although previous studies[26] have used values of σ_v as low as 0.1, while other researchers[27] suggest adiabatic conditions ($\sigma_v = 0$). The model is made of stainless steel, for which Black et al.[28] measure values of either $1.0 \pm 0.2 \times 10^{-3}$ or $1.2 \pm 0.3 \times 10^{-3}$. In our calculations we use 0.5 and 1.0×10^{-3} for σ_v to assess the effect of vibrational energy accommodation. The high value of σ_v results in nearly complete vibrational accommodation, whereas the low value is effectively an adiabatic condition near the cone tip. Based on theory and measurements, the lower value is more accurate.

Results

In the preceding sections we quantified the effect of nonequilibrium in the nozzle and obtained nonequilibrium freestream conditions by performing simulations of the nozzle flow. In this section we use these conditions to recompute the flows and make comparisons with the measured surface quantities. We also examine the effect of the slip boundary conditions. Finally, we investigate how small levels of test-section flow nonuniformity in the freestream affect the flow. We focus on run 35, and present more limited results for run 28.

The effect of slip at run 35 nominal conditions is shown in Fig. 5. In this computation the accommodation coefficients for velocity and temperature were 0.85, and a value of 0.5 was used for vibrational energy. We see that slip has little effect, with the largest difference being the heat transfer to the first cone, which decreases by less than 3%. Therefore, slip is not by itself responsible for the overprediction of heat transfer to the first cone.

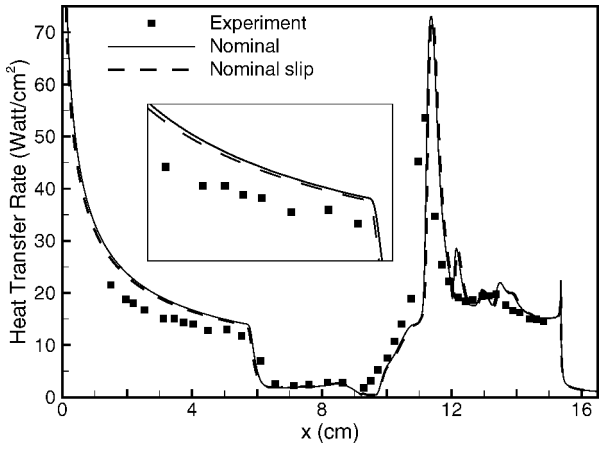

a)

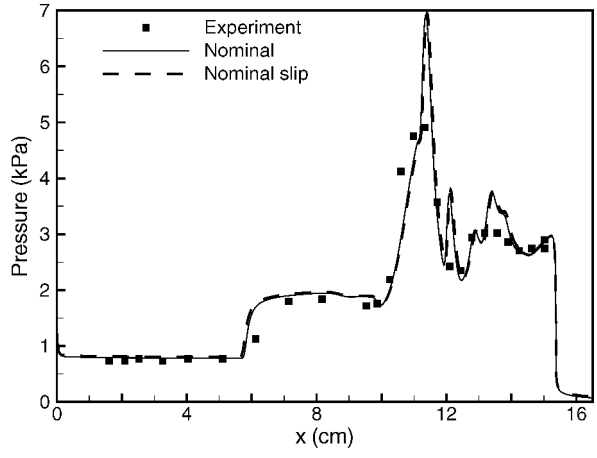

b)

Fig. 5 Heat-transfer rate and surface pressure for nominal run 35 conditions.

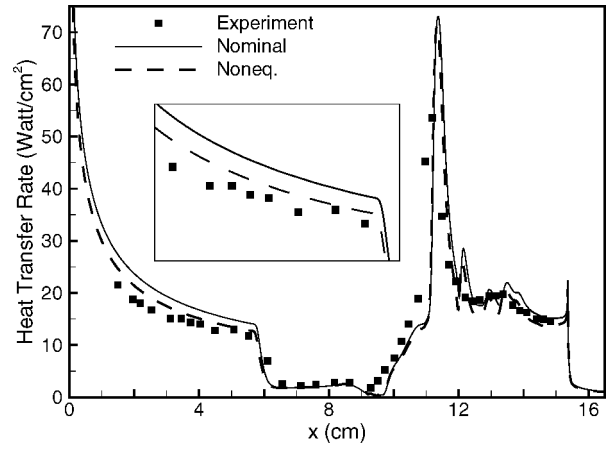

a)

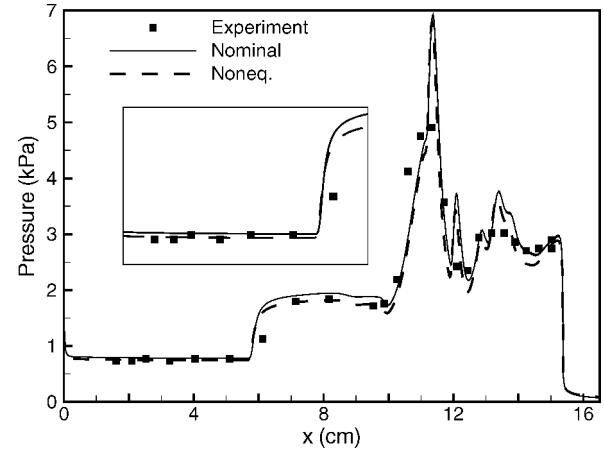

b)

Fig. 6 Heat-transfer rate and surface pressure for nonequilibrium run 35 conditions.

We observe a more significant decrease in heat-transfer rate at the first cone when the computed nonequilibrium test-section conditions are employed, as shown in Fig. 6. The heat-transfer rate decreases by 9.8% on the first cone, and the surface pressure decreases by 4.7% in that region, better matching the experimental data. The pressure in the separation zone is also reduced (by 6.3%), improving the agreement with the experiment. The separation point and the locations of the peak heat transfer and pressure do not change substantially. However, the heat-transfer rate and pressure on the last 2 cm of the second cone are reduced by 11 and 8.1%, respectively. We also employed the slip model using the nonequilibrium test-section conditions with the same accommodation coefficients. There is no significant difference in surface properties, with heat transfer being reduced by less than 2.0%. Thus, including both vibrational nonequilibrium in the nozzle and surface slip the heat transfer to the first cone is reduced by 12%, and the difference is still greater than the experimental uncertainty.

At the predicted nonequilibrium test-section conditions, the vibrational temperature is highly elevated. Therefore, the gradient of vibrational energy at the room-temperature surface is large, and the modeling of vibrational energy accommodation is important. Theory[26] and experiments[27] suggest that the vibrational energy accommodation coefficient should be much smaller than the value of 0.5 used in the previous simulations. Therefore, we simulated run 35 with the nonequilibrium conditions, and $\sigma_v = 0.001$; the results are plotted in Fig. 7. The pressure distribution and separation zone size are unaffected. But the predicted heat-transfer rate on the first cone decreases by an additional 7.0%, to within the 5% uncertainty in the data. Interestingly, the predicted heat transfer to the back half of the second cone is now below the measurements.

Clearly vibrational nonequilibrium plays an important role in these flows. It affects the test-section conditions by reducing the flux of kinetic energy. And because of weak vibrational accommodation, a large fraction of the freestream vibrational energy is not transferred to the surface.

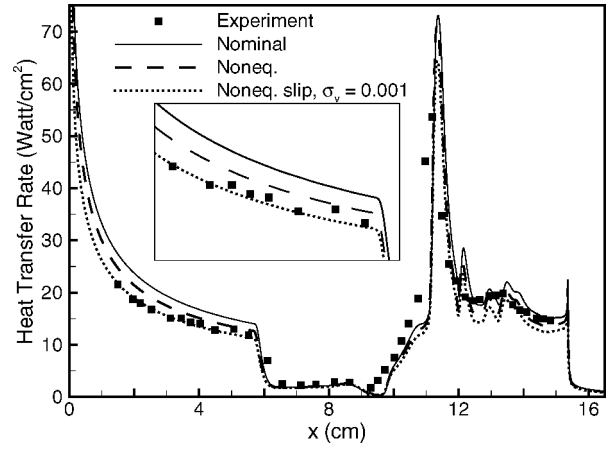

Fig. 7 Heat-transfer rate for nonequilibrium run 35 conditions and σ_v = 0.001.

An additional nonideal effect is the weak nonuniformity in the test-section flow. Figure 8 plots the computed Mach-number contours in the test section, with the double-cone flowfield superimposed at the test location. To assess the effect of the flow nonuniformity, we extract flow conditions along a line that corresponds to the location of the inflow boundary condition for the double-cone simulation. Figure 9 compares this calculation with the previous

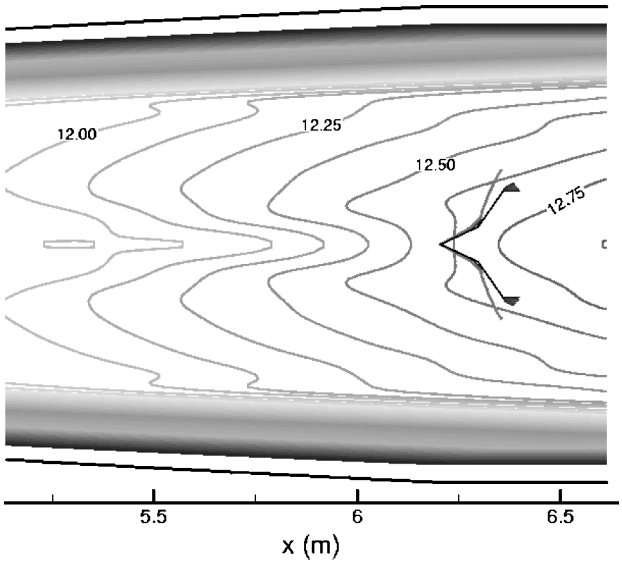

Fig. 8 Computed Mach-number contours in the test section and with double-cone flow solution superimposed.

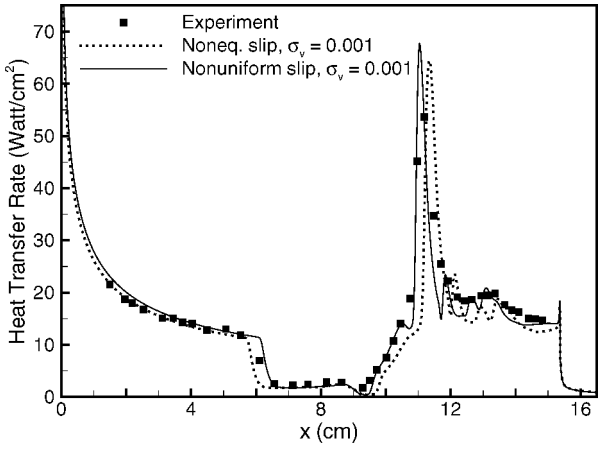

Fig. 9 Heat-transfer rate for nonuniform run 35 conditions and σ_v = 0.001.

$\sigma_v = 0.001$ result. The freestream nonuniformity reduces the size of the separation zone by 3.6 mm, shifting the heat-transfer peak upstream in better agreement with the data. Also note improved agreement on either side of the peak.

Now consider the analysis of run 28. At nominal test conditions slip has little effect, as in run 35. Figure 10 shows that when we use the computed nonequilibrium test-section conditions the heat-transfer rate to the first cone is reduced by just 2.1%, which is consistent with the small (2.6%) reduction in the kinetic energy flux for this case. Figure 10 also shows that the nonequilibrium conditions produce a significantly larger separation zone, apparently worsening the agreement with experiment. Figure 11 shows that vibrational energy slip decreases the heat-transfer rate by 11%, bringing it within about 8.7% of the measurements. However, the size of the separation zone increases. Figure 12 shows the effect of test-section nonuniformity for run 28. The simulations now agree well with the data, because of a smaller predicted separation zone and a slightly reduced heat-transfer rate to the first cone.

These results show that including vibrational energy freezing in the nozzle, weak vibrational accommodation to the model surface, and test-section nonuniformity gives excellent agreement between computations and experiments. These experiments were run in pure nitrogen at low pressures, which tends to enhance the effects of vibrational nonequilibrium. Also the nonuniformity of the test section is likely increased by the low pressure conditions, which result in thicker boundary layers and nonideal nozzle performance.

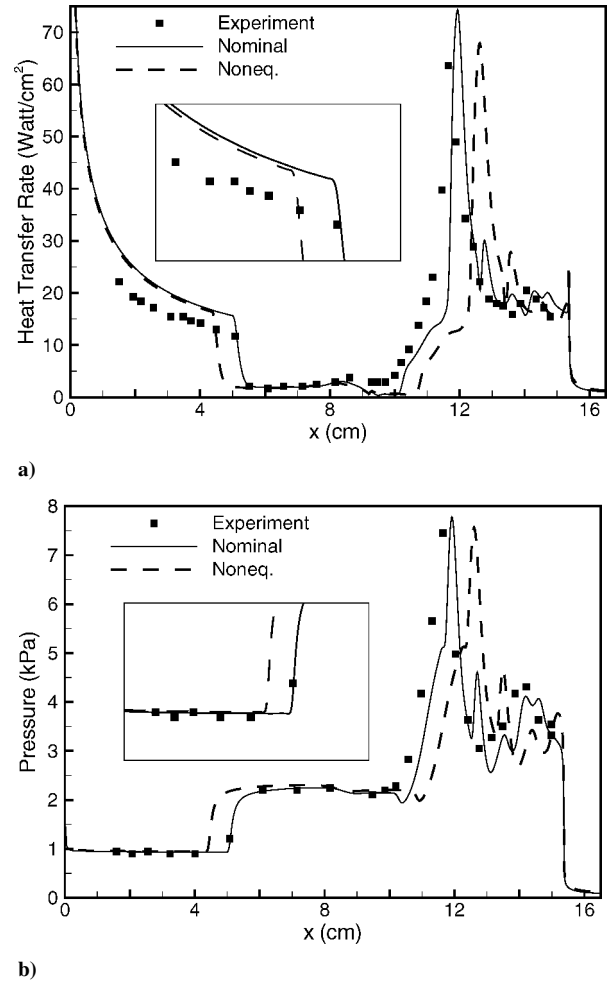

Fig. 10 Heat-transfer rate and surface pressure for nonequilibrium run 28 conditions.

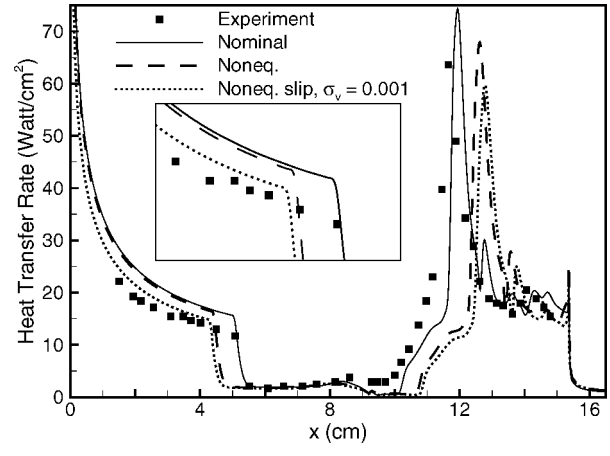

Fig. 11 Heat-transfer rate for nonequilibrium run 28 conditions and σ_v = 0.001.

Therefore, it is likely that under the usual operating conditions of the LENS facility (air at orders of magnitude larger pressure) these effects will be diminished. However further studies are required to quantify this statement.

Effect of Grid Resolution

In this section we discuss the effect of grid resolution on the double-cone flows and show that if the flowfield is underresolved it is possible to obtain good agreement with experiments for the wrong reason. The computations presented in the preceding section are

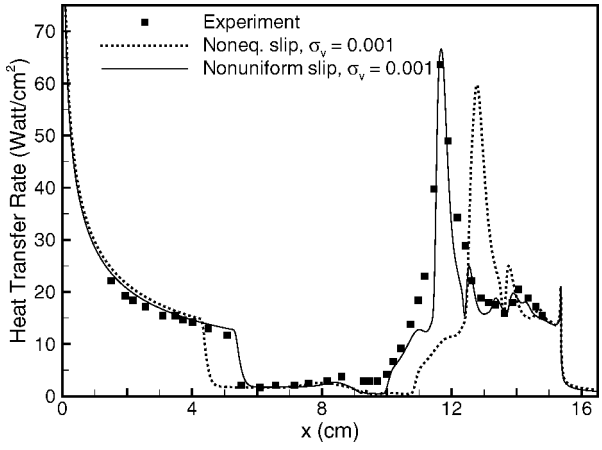

Fig. 12 Heat-transfer rate for nonuniform run 28 conditions and σ_v = 0.001.

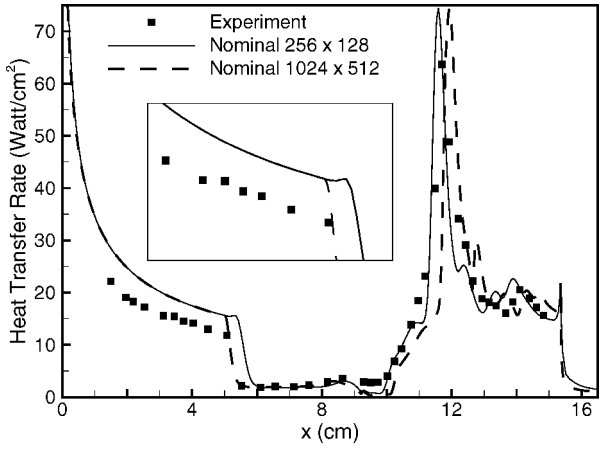

a)

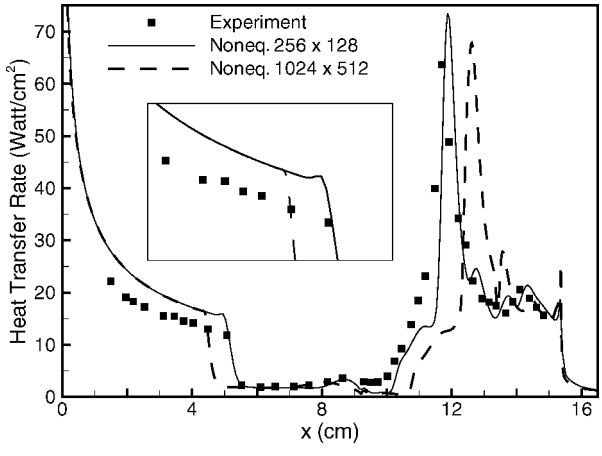

b)

Fig. 13 Heat transfer rate for a) nominal and b) nonequilibrium run 28 conditions computed on the coarse grid (256 × 128).

computationally demanding because the recirculation zone develops slowly and a large physical time must be simulated to reach steady state. In addition, large finely spaced grids must be used to ensure grid-converged results. For example, to capture the initial boundary-layer growth at the cone tip our first grid point is located 0.12 μm from the surface.

Let us study how the solution varies when the flow is underresolved. Figure 13 plots the heat-transfer rate for the nominal and nonequilibrium conditions for run 28 using a 256 × 128 grid. The coarse-grid solutions produce smaller separation zones, and as a result the nonequilibrium calculation appears to give the "correct" extent of separation. However, Fig. 14 shows that when we include the additional effects of small vibrational energy accommodation and flow nonuniformity, the coarse grid no longer agrees so well with the experiments. This is an excellent illustration of the importance of performing a rigorous grid-convergence study, preferably without knowledge of the data.

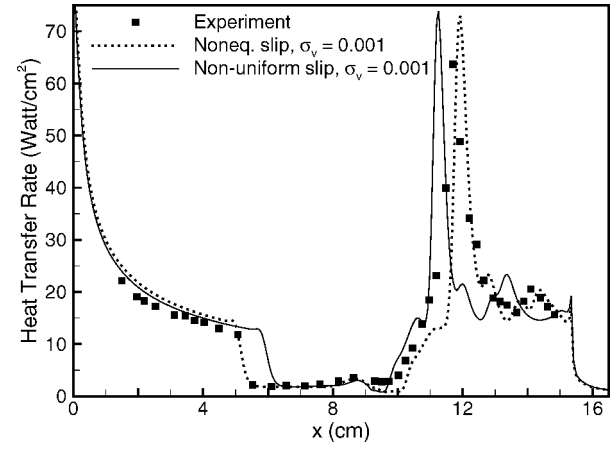

Fig. 14 Heat-transfer rate for nonuniform run 28 conditions with σ_v = 0.001 computed on the coarse grid (256 × 128).

Conclusions

We present a computational analysis of the hypersonic laminar flow of nitrogen over double-cone geometries. Initial comparisons with experimental data from Holden[4] showed a 20% overprediction of the heat-transfer rate to the first cone. We investigate the source of this discrepancy by including the effects of vibrational nonequilibrium, slip at the model surface, and weak flow nonuniformity in the test section. We simulate the flow within the facility nozzle and find that under the low pressure conditions of the experiment the vibrational energy freezes near the throat temperature. This reduces the kinetic energy flux in the nozzle test section, reducing the heat transfer to the model. However, the heat-transfer rate is still overpredicted. Therefore, we consider the failure of the no-slip boundary condition at the model surface. We find that the computed heat-transfer rate is sensitive to the vibrational energy accommodation coefficient. Using experimental values and recent theoretical results for vibrational accommodation, the heat transfer to the first cone is predicted to within the 5% measurement uncertainty. Finally, we use the results of our nozzle flowfield predictions as inflow to the double-cone flow solution. These simulations account for small levels of flow nonuniformity in the test section and show an improvement in the size of the separation zone and the heat transfer to the second cone.

The double-cone simulations also illustrate the importance of conducting careful grid-convergence studies. Because the computed separation zone size depends on the grid resolution, it is possible to obtain spurious "agreement" with experiments caused by poor grid resolution and inadequate modeling of the flow physics. Thus, the double-cone flow is a stringent CFD validation test case because it is highly sensitive to the physical models and to the quality of the numerical simulation.

Acknowledgments

This work was sponsored by the U.S. Air Force Office of Scientific Research (AFOSR) under Grant F49620-01-1-0088. The views and conclusions contained herein are those of the authors and should not be interpreted as necessarily representing the official policies or endorsements, either expressed or implied, of the AFOSR or the U.S. Government. This work was also sponsored by the U.S. Army High Performance Computing Research Center under the auspices of the U.S. Department of the Army, Army Research Laboratory cooperative agreement number DAAD191-01-2-0014, the content

of which does not necessarily reflect the position or the policy of the government, and no official endorsement should be inferred. Part of the computer time was provided by the University of Minnesota Supercomputing Institute. We thank Sergey Macheret of Princeton University, Princeton, New Jersey, for his guidance concerning vibrational energy accommodation.

References

[1]Wright, M. J., Sinha, K., Olejniczak, J., Candler, G. V., Magruder, T. D., and Smits, A. J., "Numerical and Experimental Investigation of Double-Cone Shock Interactions," *AIAA Journal*, Vol. 38, No. 12, 2000, pp. 2268–2276.

[2]Olejniczak, J., Candler, G. V., and Hornung, H. G., "Computation of Double-Cone Experiments in High Enthalpy Nitrogen," AIAA Paper 97-2549, June 1997.

[3]Olejniczak, J., Candler, G. V., Wright, M. J., Leyva, I., and Hornung, H., "An Experimental and Computational Study of High Enthalpy Double-Wedge Flows," *Journal of Thermophysics and Heat Transfer*, Vol. 13, No. 4, 1999, pp. 431–440.

[4]Holden, M. S., "Experimental Studies of Laminar Separated Flows Induced by Shock Wave/Boundary Layer and Shock/Shock Interaction in Hypersonic Flows for CFD Validation," AIAA Paper 2000-0930, Jan. 2000.

[5]Candler, G. V., Nompelis, I., and Holden, M. S., "Computational Analysis of Hypersonic Laminar Viscous-Inviscid Interactions," AIAA Paper 2000-0532, Jan. 2000.

[6]Holden, M. S., and Wadhams, T. P., "Code Validation Study of Laminar Shock/Boundary Layer and Shock/Shock Interactions in Hypersonic Flow. Part A: Experimental Measurements," AIAA Paper 2001-1031, Jan. 2001.

[7]Harvey, J. K., Holden, M. S., and Wadhams, T. P., "Code Validation Study of Laminar Shock/Boundary Layer and Shock/Shock Interactions in Hypersonic Flow. Part B: Comparison with Navier–Stokes and DSMC Solutions," AIAA Paper 2001-1031, Jan. 2001.

[8]Gnoffo, P. A., "CFD Validation Studies for Hypersonic Flow Prediction," AIAA Paper 2001-1025, Jan. 2001.

[9]Gaitonde, D., Canupp, P. W., and Holden, M. S., "Heat Transfer Predictions in a Laminar Hypersonic Viscous/Inviscid Interaction," *Journal of Thermophysics and Heat Transfer*, Vol. 16, No. 4, 2002, pp. 481–489.

[10]Candler, G. V., Nompelis, I., and Druguet, M.-C., "Navier–Stokes Predictions of Hypersonic Double-Cone and Cylinder-Flare Flow Fields," AIAA Paper 2001-1024, Jan. 2001.

[11]Roy, C. J., Gallis, M. A., Bartel, T. J., and Payne, J. L., "Navier–Stokes and Direct Simulation Monte Carlo Predictions for Laminar Hypersonic Separation," *AIAA Journal*, Vol. 41, No. 6, 2003, pp. 1055–1063.

[12]Park, C., "Assessment of Two-Temperature Kinetic Model for Ionizing Air," *Journal of Thermophysics and Heat Transfer*, Vol. 3, No. 3, 1989, pp. 233–244.

[13]Vincenti, W. G., and Kruger, C. H., *Introduction to Physical Gas Dynamics,* Krieger, Malabar, FL, 1965, pp. 198–206.

[14]Millikan, R. C., and White, D. R., "Systematics of Vibrational Relaxation," *Journal of Computational Physics*, Vol. 39, 1953, pp. 3209–3213.

[15]Blottner, F. G., Johnson, M., and Ellis, M., "Chemically Reacting Viscous Flow Program for Multi-Component Gas Mixtures," Sandia Labs., SC-RR-70-754, Albuquerque, NM, 1971.

[16]Wilke, C. R., "A Viscosity Equation for Gas Mixtures," *Journal of Chemical Physics*, Vol. 18, 1950, pp. 517–519.

[17]Wright, M. J., Bose, D., and Candler, G. V., "A Data-Parallel Line Relaxation Method for the Navier–Stokes Equations," *AIAA Journal*, Vol. 36, No. 9, 1998, pp. 1603–1609.

[18]MacCormack, R. W., and Candler, G. V., "The Solution of the Navier–Stokes Equations Using Gauss-Seidel Line Relaxation," *Computers and Fluids*, Vol. 17, No. 1, 1989, pp. 135–150.

[19]Candler, G. V., and MacCormack, R. W., "The Computation of Hypersonic Ionized Flows in Chemical and Thermal Nonequilibrium," *Journal of Thermophysics and Heat Transfer*, Vol. 5, No. 3, 1991, pp. 266–273.

[20]Druguet, M.-C., Candler, G. V., and Nompelis, I., "Simulations of Viscous Hypersonic Double-Cone Flows: Influence of Numerics," AIAA Paper 2003-3548, June 2003.

[21]Gaitonde, D. V., Canupp, P. W., and Holden, M. S., "Heat Transfer Predictions in a Laminar Hypersonic Viscous/Inviscid Interaction," *Journal of Thermophysics and Heat Transfer*, Vol. 16, No. 4, 2002, pp. 481–489.

[22]Baldwin, B. S., and Lomax, H., "Thin Layer Approximation and Algebraic Model for Separated Turbulent Flows," AIAA Paper 78-257, Jan. 1978.

[23]Candler, G. V., and Perkins, J. N., "Effects of Vibrational Nonequilibrium on Axisymmetric Hypersonic Nozzle Design," AIAA Paper 91-0279, Jan. 1991.

[24]Schaaf, S. A., and Chambre, P. L., *Flow of Rarefied Gases*, Princeton Univ. Press, Princeton, NJ, 1966, pp. 34, 35.

[25]Gökçen, T., "Computation of Hypersonic Low Density Flows with Thermochemical Nonequilibrium," Ph.D. Dissertation, Dept. of Aeronautics and Astronautics, Stanford Univ., Stanford, CA, June 1989.

[26]Boyd, I. D., Phillips, W. D., and Levin, D. A., "Sensitivity Studies for Prediction of Ultra Violet Radiation in Nonequilibrium Hypersonic Bow-Shock Waves," *Journal of Thermophysics and Heat Transfer*, Vol. 12, No. 1, 1998, pp. 38–44.

[27]Meolans, J. G., and Graur, I. A., "Thermal Slip Boundary Conditions at the Wall in Nonequilibrium Flows," *West East High Speed Flow Fields 2002*, edited by D. E. Zeitoun, J. Périaux, J. A. Désidéri, and M. Marini, CIMNE, Barcelona, Spain, 2002, pp. 233–239.

[28]Black, G., Wise, H., Schechter, S., and Sharpless, R. L., "Measurements of Vibrationally Excited Molecules by Raman Scattering. II. Surface Deactivation of Vibrationally Excited N_2," *Journal of Chemical Physics*, Vol. 60, No. 9, 1974, pp. 3526–3536.

K. Ghia
Associate Editor